A comprehensive methodology for predicting shield support hazards for a U.S. coal mine

UNA METODOLOGÍA INTEGRAL DE PROTECCIÓN PARA PREDECIR LOS RIESGOS EN PANTALLAS DE SOPORTE PARA MINAS DE CARBÓN EN ESTADOS UNIDOS



DOI: http://dx.doi.org/10.6036/7580 | Recibido: 09/mar/2015 • Aceptado: 13/may/2015

Jingyi Cheng 1,2, Zhijun Wan 1,*, Yinlin Ji 1, Wenfeng Li 1,2, and Zhimin Wang

- ¹ School of Mines, State Key Laboratory of Coal Resources and Safe Mining, China University of Mining and Technology, Xuzhou, Jiangsu, 221116, China
- ² Department of Mining Engineering, West Virginia University, Morgantown, WV, 26506, United States
- * Corrpesonding Author, zhjwcumt@hotmail.com

RESUMEN

• La predicción de riesgos en las pantallas de soporte es importante para la seguridad y la productividad de una mina de carbón subterránea. Por eso, este estudio presenta una metodología completa para predecir los riesgos en las pantallas de soporte en una zona minera virgen. Se perforó un total de 33 pozos superficiales para cubrir el total del área minera. Todos los análisis se basaron en la resistencia general y en las propiedades físicas de los estratos por encima y por debajo de la veta de carbón B, incluyendo la propia veta B. Se utilizó el modelo modificado de bloque de techo desprendido para determinar la capacidad de carga del techo de soporte y se dibujaron los diagramas isópacos de la carga del techo en tres alturas de perforación para mostrar la distribución de carga en esas diferentes alturas. Se empleó la ecuación de regresión para obtener la presión máxima del suelo, y los diagramas isópacos mostraron la diferencia de valores entre la resistencia de la masa rocosa y la distribución de presión del suelo. Para aclarár la tendencia de las discontinuidades geológicas y de los tipos de variaciones del techo se dibujó el diagrama estratigráfico y se discutieron sus correspondientes respuestas. Combinando la capacidad de carga del techo, la presión del suelo y las discontinuidades geológicas se ilustraron claramente los riesgos de la pantalla de soporte con un mapa de riesgos. La metodología propuesta puede predecir los riesgos potenciales de la pantalla de soporte e identificar las zonas donde debe instalarse soportes suplementarios, permitiendo así a los ingenieros de minas el incorporar eficientemente en un mapa integrado de predicción de riesgos, la capacidad de carga del techo, la presión del suelo y las discontinuidades geológicas para utilizarlo en el diseño y en las estrategias suplementarias de soporte.

• Palabras clave: Predicción de riesgos en pantalla de soporte, zona minera virgen, capacidad de carga del techo, presión del suelo, diagrama estratigráfico, diagrama isópaco.

ABSTRACT

Shield support hazard prediction is significant for the safety and productivity of an underground coal mine. Hence, research should be conducted on shield support hazard prediction. Thus, this study presents a comprehensive methodology for predicting shield support hazards in a virgin mining area. A total of 33 surface boreholes were drilled to cover the general mining area. All analyses were based on the extensive strength and physical properties of strata above and below coal seam B, including coal seam B itself. The modified detached roof block model was used to determine support roof load capacity, and the roof load isopach maps for three mining heights were drawn to show the load distribution for different mining heights. A regression equation was used to obtain the maximum floor pressure, and the isopach map showed the value difference between rock mass strength and floor pressure distribution. To clarify the geological discontinuities and immediate roof type variation trend, a fence diagram was drawn, and the corresponding responses were discussed. By combining the roof load capacity, floor pressure, and geological discontinuities, shield support hazards were clearly illustrated by a hazard map. The proposed methodology can predict the potential shield support hazards and identify areas where supplementary support can be implemented, thereby enabling mining engineers to incorporate the roof load capacity, floor pressure, and geological discontinuities effectively into an integrated hazards prediction map for use in support design and supplementary support strategies.

Keywords: Shield support hazard prediction, Virgin mining area, Roof load capacity, Floor pressure, Fence diagram, Isopach map.

1. INTRODUCTION

Since the 1950s, the fully mechanized longwall mining method has been utilized in coal mines. Longwall mining has developed into a safe and productive underground mining method. In modern longwall mines, shield support has been exclusively used in the longwall panel. In recent years, one vital breakthrough in shield support is a progression toward the two-leg shield support from the four-leg ones. Another progression is the increase in shield support size and capacity. To prevent shield support hazards from occurring, considerable research on roof load calculation and floor pressure has been conducted in recent decades. Several methods [1-7] are used to determine shield roof load, which is necessary in the design of shield support load capacity. Apart from the roof load capacity, floor pressure is also a critical factor that should be considered because the base plate that may dig into the floor with insufficient floor rock mass strength. Compared with shield support load capacity, floor hazards have received limited attention [1].

However, in actual field application, only one or several boreholes are selected for the calculation. Furthermore, the stratigraphic sequence that appears in the borehole is assumed to be similar to that of the area to be studied. This assumption may result in certain errors because geological conditions often change, even over a small area.

Apart from the aforementioned factors, various geological discontinuities (anomalies) are found in the overburden of coal seams, including sandstone channels, faults, joints, hill seams, and clay veins. The occurrence of these geological discontinuities may either delay the mining operations or cause problems with shield support if ground control strategies for a particular longwall panel layout are unimplemented. For instance, the hard-to-cave roof will cause strong weighting before it breaks or strong and stormy winds when it caves [8-10]; a weak roof is prone to induce roof fall accidents [11-13]. Therefore, a good understanding of geology in the proposed longwall panels is important in modern longwall operations, in which any production delay will result in a large economic loss

For hazard prediction, there are several methods proposed by researchers in countries where modern longwall mining is employed [14-19]. However, in the previous studies, the hazard maps focused more on ground control problems of entries than longwall panel support. Moreover, they were applied in mines in process not in a virgin area.

The current paper presents a comprehensive methodology to predict potential shield support hazards in a virgin mining area. The detached roof block method was utilized to calculate roof load capacity because this method has been one of the commonly used methods [19]. For the floor pressure under the support base plate, Peng regarded the base plate to be rigid and presented the floor pressure distribution by using math-

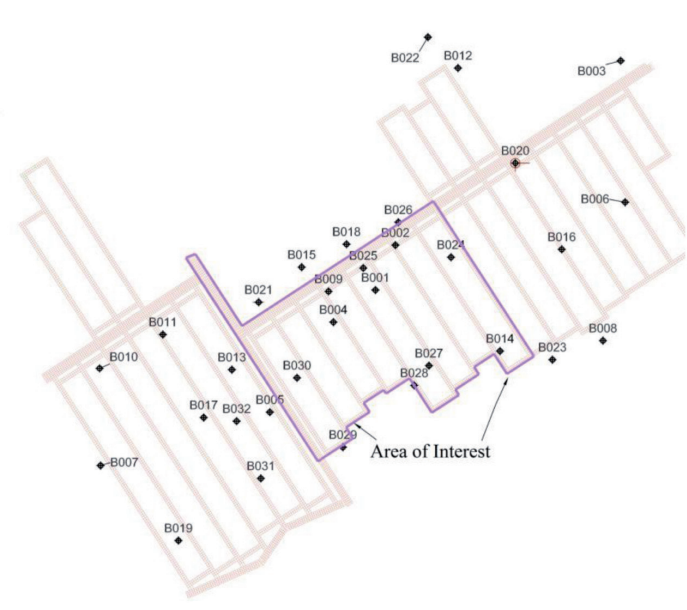


Fig. 1. Borehole locations, area of interest, and proposed longwall panel layout

ematical and mechanical analyses. To simplify, based on the finite element computer analysis, Peng developed a regression equation to determine the maximum floor pressure using three factors, i.e., the Young's Modulus of the floor material, the vertical resultant load, and the contact width between the plate and the floor along the faceline direction [19]. The latter was adopted for the floor pressure analysis in the present paper. Regarding geological analysis, several techniques can be used to predict the existence of the geological discontinuities. These techniques include the fence diagram, roof stability map, underground geological mapping, and geophysical methods. A few of these techniques, i.e., underground geological mapping and geophysical methods, may be inapplicable for the coal mine studied in this paper because the coal mine is a virgin area with no underground development yet. Therefore, the fence diagram technique was performed to identify and locate the potential geological discontinuities. Then, the roof load capacity, floor pressure, and geological discontinuities were incorporated to indicate shield support hazards by a hazard map.

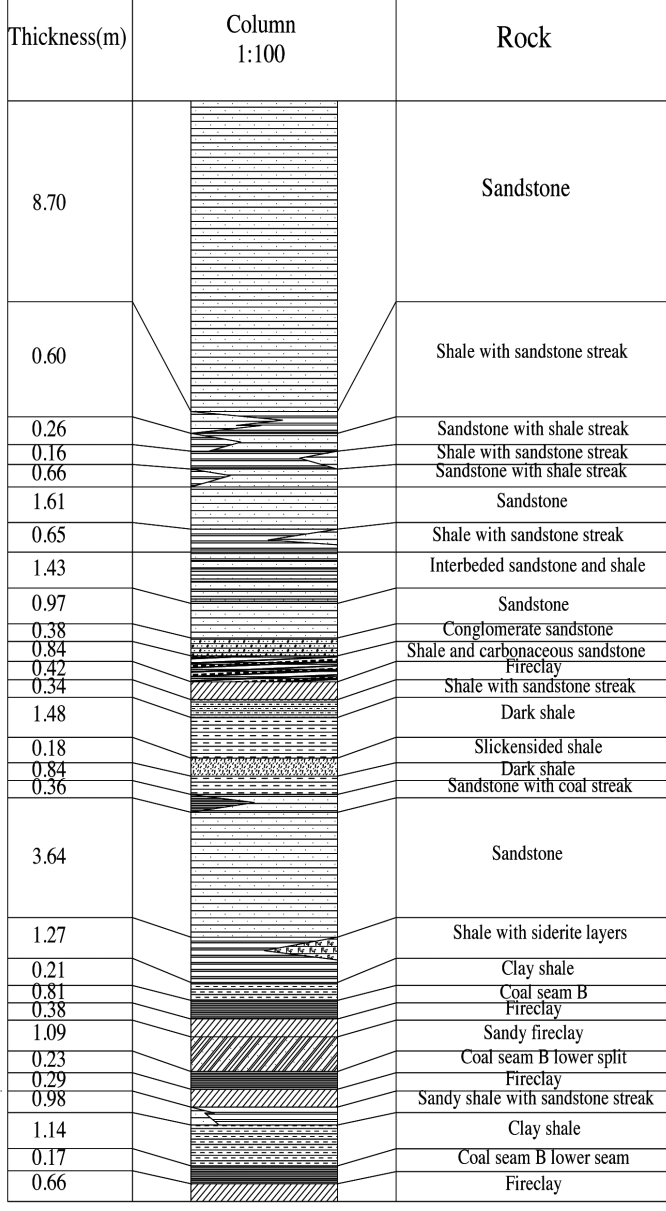


Fig. 2. Geologic column of borehole B004

2. SITE DESCRIPTION

The mine A is an underground longwall mine designed to extract the coal seam B, which is located in eastern United States. For this virgin coal mine, 33 surface boreholes were drilled for geology detection. Laboratory tests on rock core specimens from 12 boreholes were conducted to obtain mechanical and physical strength and physical properties of strata above or below the coal seam B including the coal seam B itself. A total of 1136 tests were performed for Uniaxial compressive strength (UCS), Brazilian tensile, slake durability, and point load index test. The tensile strengths were used in the following roof load calculation and the subsequent floor pressure analyses utilized the data on UCSs, moduli, and slake durability. The data from core logs revealed that the overburden depth of coal seam B varies from 54.56 m to 476.7 m thick and the thickness of coal seam B varies from 0.15 m to 1.73 m within the proposed longwall mining area. Core logs in the area of interest indicated that the thickness of the coal seam B varies from 0.63 m to 1.27 m and seam dips are less than 3.0 degrees. Fig. 1 shows the proposed longwall panel layout, area of interest, and borehole locations. In this paper, we concentrated on the area of interest. Fig. 2 is the geologic column of borehole B004 which is within the area of interest.

3. SHIELD SUPPORT LOAD CAPACITY DETERMINATION

The two-leg shields have been exclusively used in U.S. longwall mining since the early 1990s, and adopted to be used in modern high-production and high-efficiency longwalls all over the world. Therefore, two-leg shields are recommended for the proposed longwall mining.

For the U.S. longwall mining, the modified detached roof block method has been proven to be the most applicable to calculate the shield capacity [19], hence the method is used in the present paper. Shield load capacity has been determined from 33 boreholes, which are located within the proposed longwall panels. The tensile strengths used for shield capacity determination can be estimated by multiplying the lab-determined values by reduction factors. To be clearer, reduction factors used in this study for different kinds of rock are listed in table 1 which refers to Sys S. Peng's recommendation in reference [19].

Rock	Reduction factor
Coal, claystone, or fireclay	0.2
Shale or mudstone	0.3
Snadstone, siltstone, limestone, or laminated sandstone	0.4
Massive sandstone	0.6

Table 1 Reduction factors used in this study for defferent kinds of rock

The average values of similar kinds of rock types are applied for a specific rock type, because the strength of similar types of rocks at similar elevations between different boreholes is closer to each other.

The modified detached roof block model is shown in Fig. 3. In this model, each individual stratum in the roof is consid-

ered to be a cantilever beam with fixed-end point at the coal face. In the shield load calculation, the self-supporting length of each beam is initially determined, and then summarized to obtain the total load on the shield using the following equations

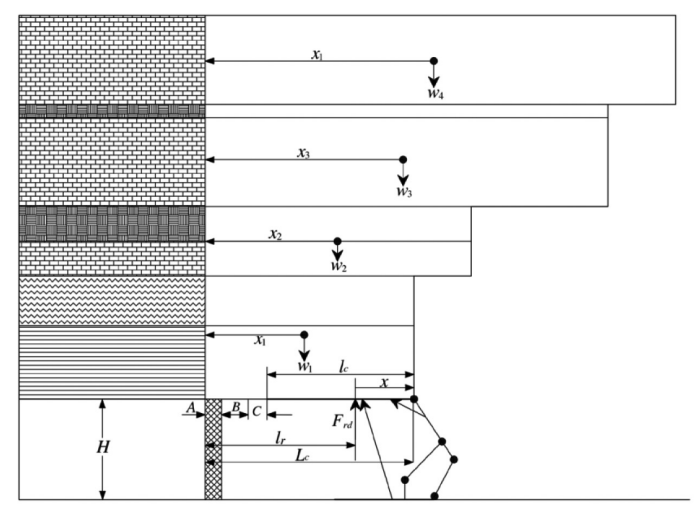


Fig. 3. Cantilevered beam roof loading model [19]

To calculate the length of a fix-ended cantilevered beam:

$$L_b = t \sqrt{\frac{T_0}{3q}} \tag{1}$$

To calculate the distance from the end of canopy to the first supporting point of the coal face:

$$L_c = A + B + C + l_c \tag{2}$$

To claculate the resultant force:

$$F_{rd} = (DF) \frac{\sum_{i=1}^{k} W_i x_i}{l_r}$$
(3)

To calculate the weight of the *i*th rock layer:

$$W_i = L_{bi} St_i \gamma_i \tag{4}$$

To calculate the distance from the center of gravity of the i^{th} rock layer to the first supporting point of the coal face:

$$x_i = \frac{L_i}{2} \tag{5}$$

where DF is the design factor, generally 1.10 to 1.25, with 1.25 adopted here for security; k is the number of rock layers within the required caved zone; L_b is the length of the fixended cantilevered beam; L_{bi} is the length of the cantilevered beam of the i^{th} rock layer (or beam); q is the uniform load on the beam per unit length and is equal to γgh , where γ is the average density of overburden strata, and S is the support spacing at 1.75 m; t_i is the thickness of cantilevered beam of the i^{th} rock layer (or beam); T_0 is the in-situ tensile strength of the rock beam; x_i is the distance from the center of gravity of

the ith rock layer (or beam) to the first supporting point of the coal face; w_i is the weight of the i^{th} rock layer (or beam); γ_i is the density of the i^{th} rock layer (or beam); L_c is the length of shield canopy, 4.52 m; A is the web width, 1.07 m; B+C is the unsupported distance, 0.52 m; L_r is the distance from the face line to the shield's hydraulic legs, 4.94 m; and F_{rd} is the resultant load on shield.

The assumptions of common parameters used in this model are listed in Table 2.

Assumptions	Value	
In-situ vertical rock pressure, MPa/m	0.0254	
Shield width, m	1.75	
Length of the shield canopy, m	4.53	
Web width, m	1.07	
Unsupported distance, m	0.52	
Distance from the face line to the shield's leg, m	4.94	
Angle of the shield leg from the horizontal, degree	65	
Design Factor (DF)	1.25	
Bulking Factor	1.125	
Width of shield base plate, m	1.6	

Table 2 Assumptions for shield capacity calculation

If an individual roof beam does not overhang, i.e., its length is less than L_c (Fig. 3), the weight of the beam is calculated for the full beam length of L_c and the beam rests fully on the first underlying cantilevered beam. Therefore, in the process of calculation, if the self-supporting length of the No. 1 roof beam, L_p , is less than L_c , the No. 1 roof beam length is assumed to be L_c . Using this method, the shield support capacity required will depend on the stratigraphic sequence, and each of which will require a different support capacity because of the different beam length and beam sequence in the roof.

Current longwall face equipment in the United States dictates that the minimum mining height is 1.68 m (5.5 ft). However, the above information on the coal seam B in the area of interest shows that the thickness of the coal seam varies from 0.63 m to 1.27 m. Thus, the shearer will cut either the roof or floor or both. To keep the roof and floor stable, all the core logs from exploration boreholes are utilized to determine the cutting horizon. The mining height range is 1.74 m to 2.19 m, and most boreholes requiring mining heights are within the range of 1.83 m to 2.13 m.

For analysis, shield capacity of three mining heights, namely, 1.83, 1.98, and 2.13 m (6, 6.5, and 7 ft) was separately calculated. The height (or thickness) of the modified detached roof block is controlled by the bulking factor of the roof strata. The conservative average bulking factor is 1.125, i.e., the height after caving is eight times the mining height (14.63 m for mining height of 1.83 m, 15.85 m for mining height of 1.98 m, and 17.07 m for mining height of 2.13 m). In the calculation process, the roof load or the required shield support load capacity is determined borehole by borehole.

The results show that, for all the 33 boreholes, when mining heights are 1.83, 1.98, and 2.13 m, the required support load capacity ranges from 512 tons (B209) to 1,384 tons (B020), from 555 tons (B016) to 1,384 tons (B020), and from 597 tons (B001) to 1.384 tons (B020), respectively.

Fig. 4 shows the frequency distribution of the required leg yield load for the three mining heights. When mining height is 1.83 m, 24 boreholes in the load range from 500 tons to 599 tons are required, whereas only 2 boreholes when mining height is 2.13 m. When mining height is 1.98 m, the load range of 600 tons to 699 tons accounts for a large proportion (19 boreholes or 58%). When mining height is 2.13 m, a great majority of the support load capacity required are in the range from 600 tons to 799 tons, which is approximately 78% (or 26 boreholes) of the total number of boreholes.

Based on the results, for all three mining heights, the required shield yield load for borehole B020 is the largest. The extra-large roof loading can be attributed to the fact that borehole B020 is located in the shallow cover area and a very thick (7.56 m) sandstone stratum exists within the caving height of concern. After mining, this sandstone stratum will overhang more than 11.28 m before caving (calculating from the borehole data), producing a very large additional weight on the shield. Similar reasoning applies to boreholes B021 and B018 when mining height is 1.98 m.

The 1.75 m wide two-leg shields are recommended for the proposed longwall mining. The modified detached roof block method was used to calculate the shield capacity of 33 boreholes for three mining heights (1.83, 1.98, and 2.13 m). Considering all factors, the two-leg shields are recommended to have a yield load of 900 tons, which will cover all areas except that around borehole B020.

Mining height of 2.13 m will induce much higher support load when compared with mining heights of 1.83 and 1.98 m. Moreover, high mining height will increase rock content. The resultant loads obtained are used in the following computation of floor pressure, and the load of mining height of 1.98 m is relatively higher than that of the mining height of 1.83 m. Hence, mining height of 1.98 m is selected for the following floor pressure analysis.

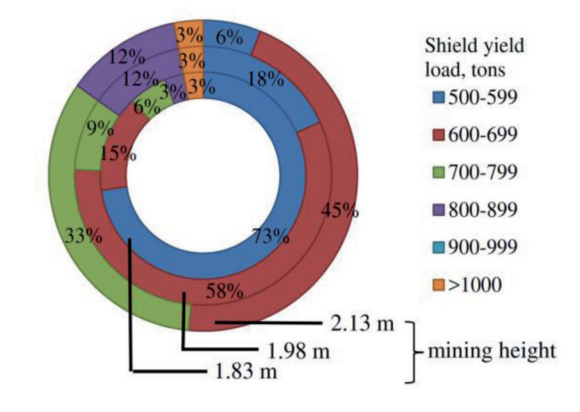


Fig. 4. Frequency distribution of the required shield yield load (tons)

Fig. 5, Fig. 6, and Fig. 7 show the isopach maps of the required yield load distributions for the mining heights of 1.83, 1.98, and 2.13 m, respectively. In the shield capacity isopach map (tons) of three mining heights, different colors are ap-

plied to indicate the roof load hazards along the longwall retreating direction. In the high load pressure area, support crush accidents could occur if the recommended shield yield load is adopted.

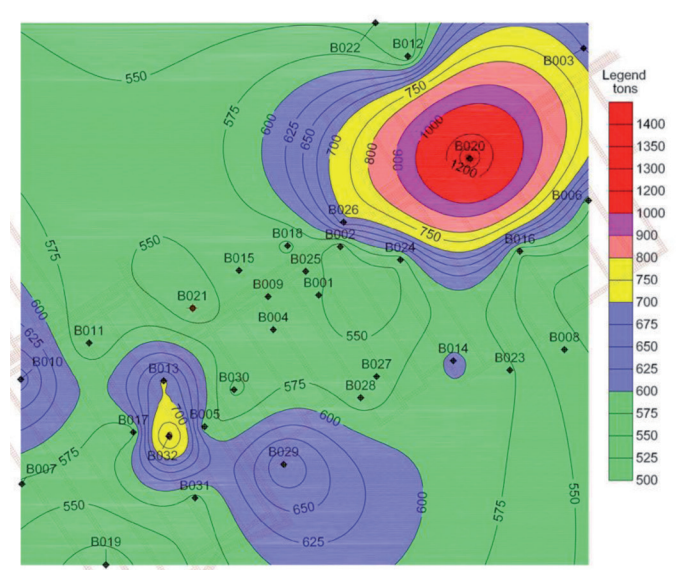


Fig. 5. Shield capacity isopach map (tons) - mining height of 1.83m

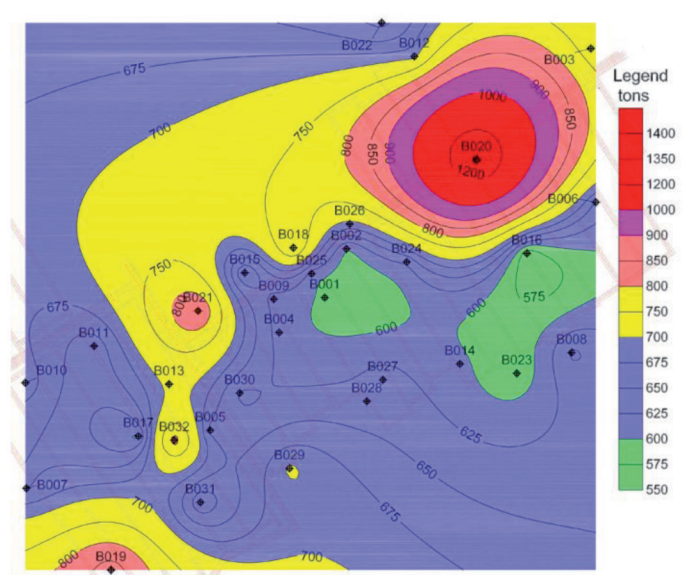


Fig. 6. Shield capacity isopach map (tons) - mining height of 1.98 m

4. FLOOR PRESSURE UNDER THE BASE PLATE

For the two-leg shields, when the immediate floor stratum is soft, the base plates of the shield may dig into the floor during operation. This phenomenon will cause difficulties in shield advance. Therefore, the bearing capacity of the immediate floor stratum must be determined hence that the shield dimensional configurations can be designed to produce a peak toe pressure less than the floor bearing capacity. Before calculating the floor pressure, the cutting horizon must be determined, which has already been known in part 3, to figure out the immediate roof type. According to the core logs of the drill holes, the immediate roof rock type of each borehole is determined.

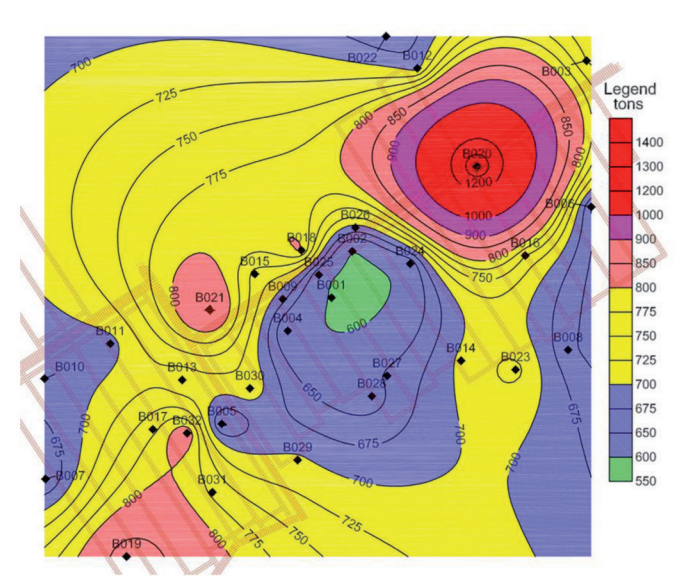


Fig. 7. Shield capacity isopach map (tons) - mining height of 2.13 m

In determining floor pressure in this section, the base plates of the shield were assumed to be elastic. Based on the finite element computer analysis, Peng developed a regression equation to determine the maximum floor pressure, which can be expressed as follows [19]:

$$p_{\text{max}} = 1233 + 213x_1 + 2.72x_2 - 38x_3, psi$$
 (6)

where x_i is the Young's Modulus of the floor material in 10^6 psi $(10^6$ psi = 6.895 GPa), x_2 is the vertical resultant load in tons, and x_0 is the contact width between the plate and the floor along the faceline direction in inches (1 inch = 2.54 cm).

Three factors: Young's modulus of the floor rock, vertical resultant force, and the contact width between the base plate and the floor, were used to analyze the floor pressure. The Young's Modulus of the floor rock was obtained from the rock property tests for this project. The vertical resultant force from the modified detached roof block method was used, and the contact width between the base plate and the floor was assumed to be 1.60 m.

Table 3 shows the partial results of floor pressure determination. The majority of the immediate floor strata are sandy shale, sandy shale with sandstone streaks, shale, shale with sandstone streak(s), and shale with coal streak(s). Because the in-situ bearing capacity of the floor rocks was unavailable, the UCSs of the floor rocks were used to estimate their floor bearing capacities by linear reduction method. For safety reason, the reduction factor of 5 for rock strength was adopted. The results demonstrate that the selected floor strata of mining horizon within the area of interest are weak; hence, not enough to prevent shields from digging into the floor. Notably, fireclay and sandy fireclay are usually hard and firm when dry, but becomes soft and muddy when wet. Hence, to keep the floor as dry as possible is important, especially when the rock type is fireclay. Meanwhile, the slake durability tests of these floor rocks indicated that these floor rocks are resistant to water. Moreover, these floor rocks contain little clay materials, thereby resisting water weathering. The shield support floor pressure isopach map using different values between rock strength and maximum floor pressure is shown in Fig. 8.

The isopach map of differential values (i.e., difference between the maximum floor pressure and rock mass strength) for mining height of 1.98 m (Fig. 8) can be used to clarify the potential area where the shield base tends to sink into the floor. Cross-section #4 is located slightly outside, but oriented along the proposed setup rooms. Therefore, the proposed fence diagrams will show the geological differences among the different panels. These laboratory data can be used to validate the

Boreholes	Rock Type of Immediate Floor	Uniaxial Compressive Strength (UCS)*, MPa	Rock Mass Strength (UCS/5, MPa)	Young's Modulus [*] , GPa	Maximum Floor Pressure (Mining Height 1.83 m), MPa
B002	Sandy fireclay	76.96	15.39	2.23	6.47
B003	Shale with coal streak(s)	24.84	4.97	0.78	6.72
B004	Sandy fireclay	38.74	7.75	1.02	5.05
B005	Shale with sandstone streak(s)	40.03	8.01	1.24	5.83
B006	Black shale	45.88	9.18	1.62	6.51
B007	Shaley sandstone	106.03	21.21	2.51	7.84
B008	Fireclay	36.09	7.22	0.94	5.67
B009	Sandy shale w/sandstone streak(s)	88.23	17.65	1.16	5.35
B011	Shale with sandstone streak(s)	40.03	8.01	1.24	5.67
B012	Shale	54.74	10.95	1.26	6.79
B014	Shale with coal streak(s)	28.80	5.76	0.74	9.54
B015	Sandy shale with sandstone streak(s)	38.74	7.75	1.02	4.63
B016	Sandy shale	93.80	18.76	2.05	5.41
B017	Sandy shale with sandstone streak(s)	81.52	16.30	1.73	5.68
B018	Sandy shale with sandstone streak(s)	81.52	16.30	1.73	9.66
B019	Sandy shale	93.80	18.76	2.05	11.46
B020	Sandy shale with sandstone streak(s)	81.52	16.30	1.73	20.51
B021	Clay shale	32.21	6.44	0.79	9.27

Table 3 Partial results of floor pressure determination

NOTE: * Cores of 12 boreholes were selected for the mechanical tests. The other data were inferred from the abutment corresponding boreholes.

5. GEOLOGICAL DISCONTINUITIES ANALYSIS

The construction and its applicability in locating anomalies of a fence diagram mostly depend on the location and density of the boreholes. Thus, the closer the two adjacent boreholes are, the more accurate the lithological projection that can be made for the area between the boreholes is. For the proposed longwall panels in the area of interest, 12 boreholes have been used to construct four cross-sections to establish the fence diagram (Fig. 9). For clarity, the 3D view of the cross-section #1 is shown separately in Fig. 9(A), because it will overlap with 3D view of the cross-section #4 if all four cross-sections are plotted together in one map. Cross-sections #1, #2, and #3 are generally along the proposed longwall retreat direction. These three cross-sections will show the geological changes that are likely to be encountered during panel retreat operations.

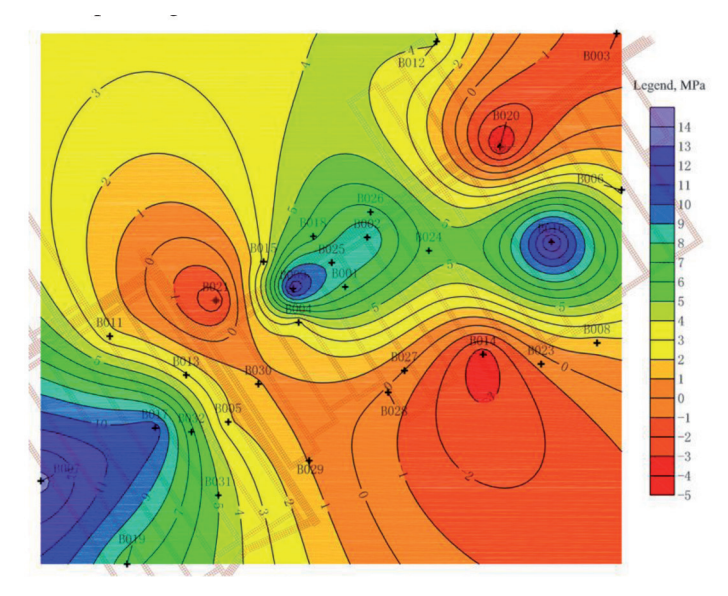


Fig. 8. Isopach map of differential values (maximum floor pressure-rock mass strength)

lithology match of the constructed fence diagrams. Considering that the proposed mining height is 1.83 m, a fence diagram covering 18.9 m to 25 m thick above the coal seam B was constructed to show the geology changes.

The three-dimensional (3D) view of the fence diagram is shown in Fig. 9, whereas the two-dimensional (2D) view of each cross-section, i.e., cross-sections #1, #2, #3, and #4, is shown in Fig. 10. The purpose of constructing the 2D cross-sections is to identify any potential geological discontinuities easily. The potential lithology changes or geological discontinuities in cross-sections #1, #2, #3, and #4 are highlighted in Fig 10(a), Fig. 10(b), Fig. 10(c), and Fig. 10(d), respectively. Generally, the immediate roof can be categorized into five types: I, massive strong and hard immediate roof: B033, B028, B014, and B030; II, strong and hard roof with medium thick: B031; III, Weak and thick roof: B021, B015, B009, B026, and B002; IV, weak and less thick roof: B029, B004, and B028; V, lithology changes and geological discontinuities: encircled in Fig. 10.

For type I, the immediate roof tends to hang for a large area before it caves, once caved, it will lead to strong wind blasts, which are harmful to the face equipment and crew. For type II, the roof breaks for a certain distance and a clear and strong periodic weighting will occur. For type III, the caved immediate roof will fully fill up the gob space and no or minor periodic weighting, and the weak and thick roof is prone to induce roof fall accidents. For type IV, the caved rock cannot fully fill up the gob area, and a large gap between the caved rock and the lower main roof exists. Hence, the main roof will induce a clear periodic weighting. For type IV, geological changes will cause hazards if no special measures were taken.

According to the distribution of immediate roof type within the fence diagram area, along the retreating direction, the immediate roof is estimated to change in the following order: I to IV to III, with type I accounting for the most part, ap-

proximately 70%; then, the immediate roof changes into type IV for a short length; finally, the face will encounter type III. A few geological discontinuities will occur all the way along the retreating direction (encircled in Fig. 10). Based on the change in the immediate roof type, a corresponding measure should be taken to avoid support accidents, such as roof fall or heavy periodic weighting, causing the support to crush.

6. HAZARD MAP DISCUSSION

The hazard map below is the combined map of the abovementioned three factors affecting shield support safety. Based on the map, the areas of higher than normal hazards that can be delineated as the roof load, floor pressure, and geological discontinuities are integrated. In Fig. 6 and Fig. 8, the roof load and floor pressure distribution are clearly shown. The potential hazardous areas combined with the geological change tendency and abnormalities (see Fig. 10) add one more level of confidence in the hazard map. Moreover, core logs in other drill holes were applied to make the prediction accurate. Based on the map, at the start of mining and the end of the area of interest, the expected large floor pressure, weak and thick immediate roof, and massive strong and hard immediate roof deserve utmost attention. Before the initiation of mining, this map can serve as a guide map for mining engineers to make the right decision on support design and supplementary support strategies.

7. CONCLUSION

A shield support hazards mapping method to predict various support hazards has been presented in this paper. Results of this study, in which roof load, floor pressure, and geological

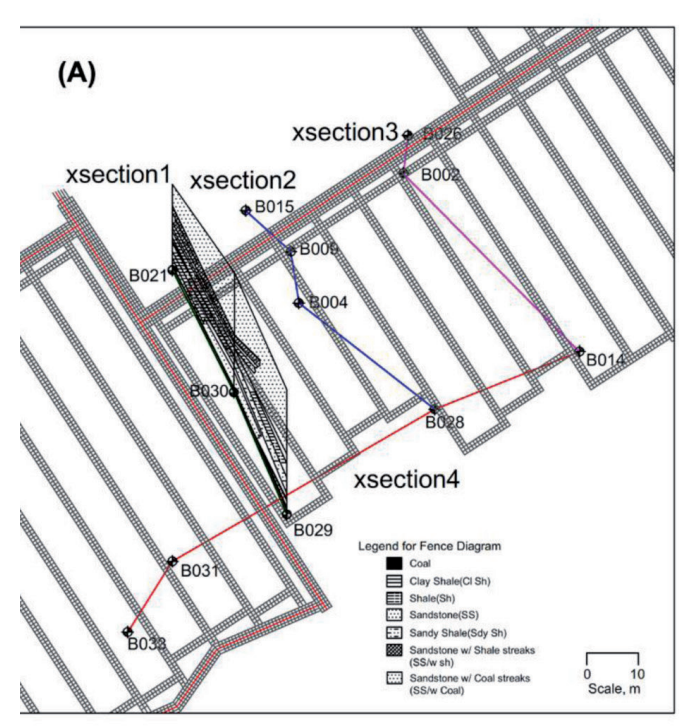
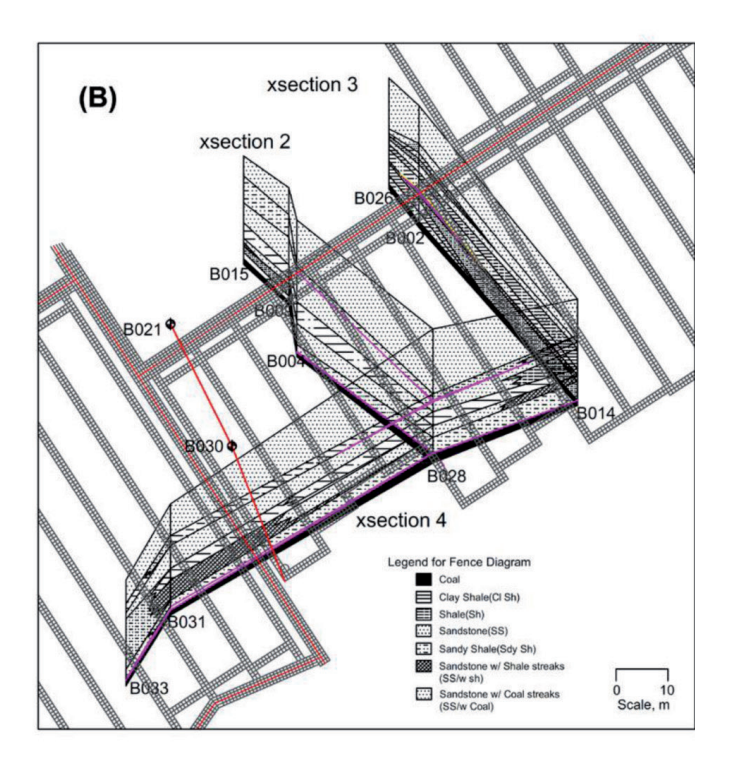


Fig. 9. 3D view of the fence diagram



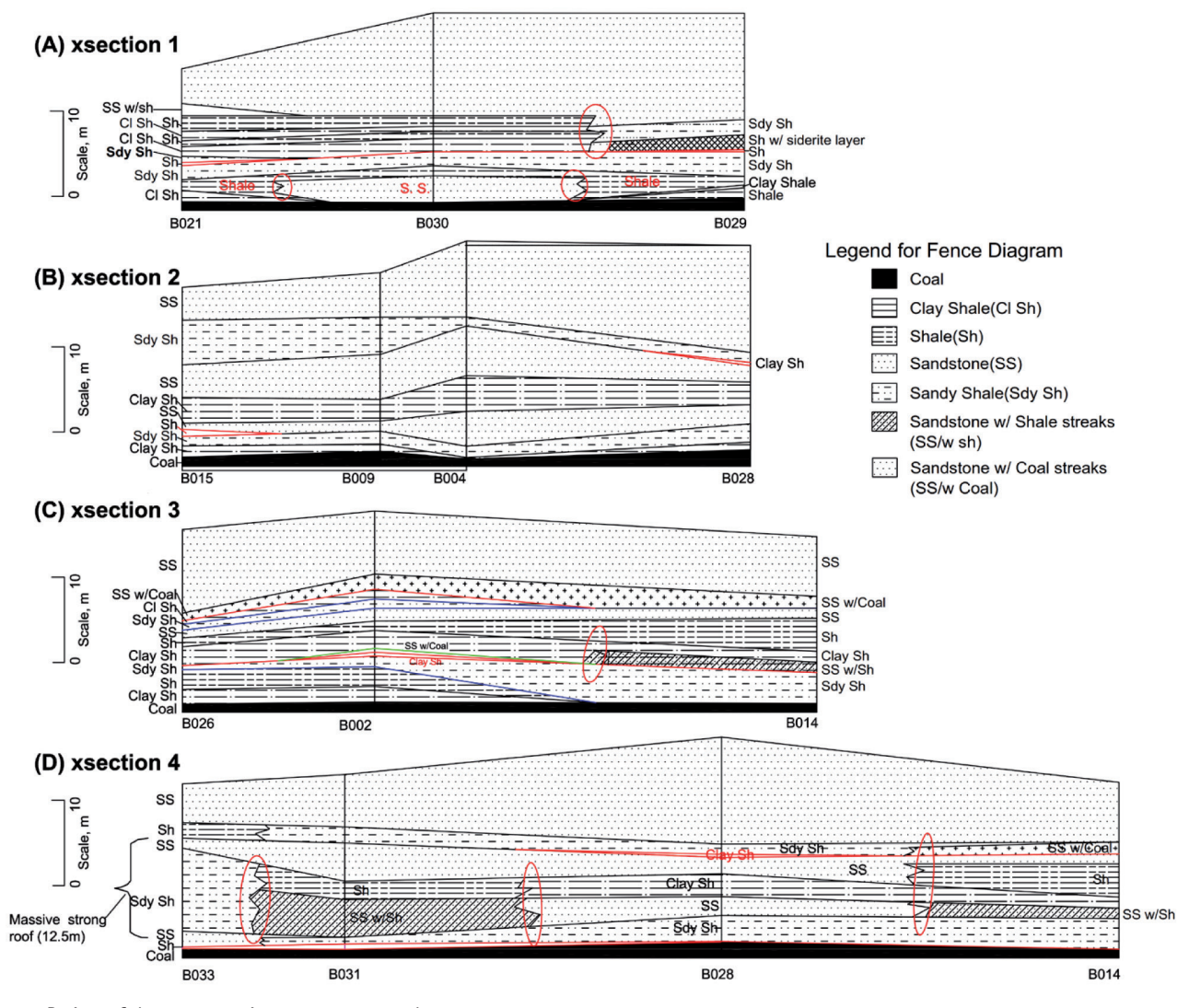


Fig. 10. 2D view of the cross-sections #1, #2, #3, and #4

discontinuities are incorporated, demonstrated a comprehensive methodology to predict potential shield support hazards in a virgin mining area. Four detailed conclusions are summarized as follows,

- 1. Because mining height of 2.13 m will induce much higher support load when compared with mining heights of 1.83 and 1.98 m, and the load of mining height of 1.98 m is relatively higher than that of the mining height of 1.83 m and higher mining hight will result in higher calculated floor pressure, mining height of 1.98 m is adopted in the following floor pressure analysis.
- 2. When the mining height is 1.98m, the isopach map of differential values between the maximum floor pressures and rock mass strengths can be used to indicate the potential area where the shield base tends to sink into the floor.
- 3. From the fence diagrams, the immediate roof is estimated to change in the following order: I to IV to III, with type I accounting for about 70%; then, the immediate roof encounters type IV for a short length; finally, the face will change into type III. Besides, geological discontinuities along the retreating direction are also shown

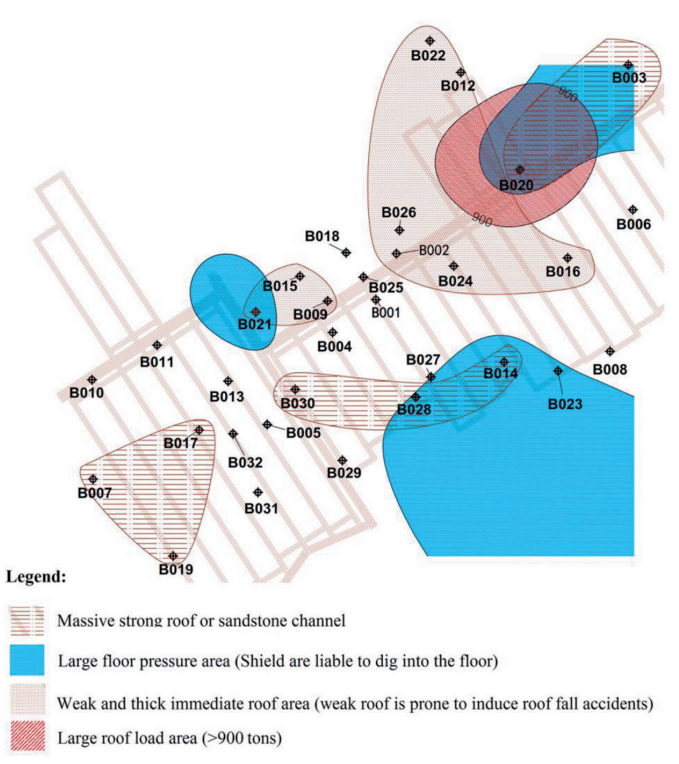


Fig. 11. Shield support hazard map

- in the fence diagrams. According to the information of the immediate roof, countermeasures should be taken to avoid roof fall or heavy periodic weighting which will cause the support to crush.
- 4. Notably, more detailed geological conditions will be available when mining begins. Therefore, this map can be modified as mining activities continue. The proposed hazard mapping approach is a promising development to figure out and understand the geological conditions for predicting shield support hazards.

ACKNOWLEDGEMENT

This study was sponsored by State Key Laboratory of Coal Resources and Safe Mining, CUMT (NO.SKLCRSM12X02), National High Technology Research and Development Program of China (NO. 2012AA062100) and the Program for New Century Excellent Talents in University of China (NO. NCET-10-0770).

BIBLIOGRAPHY

- [1] Peng SS. "Topical areas of research needs in ground control-A state of the art review on coal mine ground control". International Journal of Mining Science and Technology. In press. February 2015. DOI: http://dx.doi.org/10.1016/j. ijmst.2014.12.006
- [2] Medhurst TP, Reed K. "Ground response curves for longwall support assessment". Mining Technology. June 2005. Vol.114-2. p.81-88. DOI: http://dx.doi.org/10.1179/037178405X44575
- [3] Trueman R, Lyman G, Callan M, et al. "Assessing longwall support-roof interaction from shield leg pressure data". Mining Technology. September 2005. Vol.114-3. p.176-184. DOI: http://dx.doi.org/10.1179/037178405X53953
- [4] Trueman R, Lyman G, Cocker A. "Longwall roof control through a fundamental understanding of shield-strata interaction". International Journal of Rock Mechanics and Mining Sciences. February 2009.Vol. 46-2. p.371-380. DOI: http://dx.doi. org/10.1016/j.ijrmms.2008.07.003
- [5] Shao X, Xia Y, Shi P. "Parameter Design and Application of Hydraulic Support with Hanging Chain and Splicing Beam in Shallow Seams". Advanced Materials Research. August 2011. Vol. 317-319. p.2244-2248. DOI: http://dx.doi.org/10.4028/ www.scientific.net/AMR.317-319.2244
- [6] Singh GSP, Singh UK. "Prediction of caving behavior of strata and optimum rating of hydraulic powered support for longwall workings". International Journal of Rock Mechanics and Mining Sciences. January 2010. Vol. 47-1. p.1-16. DOI: http:// dx.doi.org/10.1016/j.ijrmms.2009.09.001
- [7] Singh GSP, Singh UK. "A numerical modeling approach for assessment of progressive caving of strata and performance of hydraulic powered support in longwall workings". Computers and Geotechnics. September 2009. Vol. 36-7. p.1142-1156. DOI: http://dx.doi.org/10.1016/j.compgeo.2009.05.001
- [8] Fan J, Dou L, He H, et al. "Directional hydraulic fracturing to control hard-roof rockburst in coal mines". International Journal of Mining Science and Technology. March 2012. Vol. 22-2. p.177-181. DOI: http://dx.doi.org/10.1016/j. ijmst.2011.08.007
- [9] Lu C, Dou L, Zhang N, et al. "Microseismic frequencyspectrum evolutionary rule of rockburst triggered by roof fall". International Journal of Rock Mechanics and Mining Sciences. December 2013. Vol. 64. p.6-16. DOI: http://dx.doi. org/10.1016/j.ijrmms.2013.08.022
- [10] Huang Q, Gao F, Zhao J. "Study on the collapse mechanism of the hard roof rocks". Advanced Materials Research.

- May 2012. Vol.524-527. p.722-725. DOI: http://dx.doi. org/10.4028/www.scientific.net/AMR.524-527.722
- [11] Hebblewhite BK, Lu T. "Geomechanical behaviour of laminated, weak coal mine roof strata and the implications for a ground reinforcement strategy". International Journal of Rock Mechanics and Mining Sciences. January 2004. Vol.41-1. p.147-157. DOI: http://dx.doi.org/10.1016/j. ijrmms.2003.08.003
- [12] Lu T, Liu Y, Xu F. "Deformation and failure of stratified weak roof strata of longwall roadway". Journal of University of Science and Technology Beijing, Mineral, Metallurgy, Material. October 2007. Vol. 14-5. p.387-394. DOI: http:// dx.doi.org/10.1016/S1005-8850(07)60077-2
- [13] Shen B. "Coal mine roadway stability in soft rock: a case study". Rock Mechanics and Rock Engineering. November 2014. Vol. 47-6. p.2225-2238. DOI: http://dx.doi. org/10.1007/s00603-013-0528-y
- [14] Wang B, Liu S, Liu J, et al. "Advanced prediction for multiple disaster sources of laneway under complicated geological conditions". Mining Science and Technology (China). September 2011. Vol. 21-5. p.749-754. DOI: http://dx.doi. org/10.1016/j.mstc.2011.03.001
- [15] Razani M, Yazdani-Chamzini A, Yakhchali SH. "A novel fuzzy inference system for predicting roof fall rate in underground coal mines". Safety science. June 2013. Vol. 55. p.26-33. DOI: http://dx.doi.org/10.1016/j.ssci.2012.11.008
- [16] Palei SK, Das SK. "Logistic regression model for prediction of roof fall risks in bord and pillar workings in coal mines: An approach". Safety science. January 2009. Vol. 47-1. p.88-96. DOI: http://dx.doi.org/10.1016/j.coal.2005.03.003
- [17] Ghasemi E, Ataei M. "Application of fuzzy logic for predicting roof fall rate in coal mines". Neural Computing and Applications. May 2013. Vol. 22-1. p.311-321. DOI: http:// dx.doi.org/10.1007/s00521-012-0819-3
- [18] Palei SK, Das SK. "Sensitivity analysis of support safety factor for predicting the effects of contributing parameters on roof falls in underground coal mines". International Journal of Coal Geology. September 2008. Vol. 75-4. p.241-247. DOI: http://dx.doi.org/10.1016/j.coal.2008.05.004
- [19] Peng SS (2008). Coal Mine Ground Control. 3rd edition. Morgantown, WV, 2008. 750 p. ISBN: 978-0-9788383-4-5